Desalination and Water Treatment
www.deswater.com

doi: 10.5004/dwt.2017.0343

60 (2017) 269–275
January

Enhanced photo-catalytic activity of CeO_2-ZnO nano-structure for degradation of textile dye pollutants in water

Mohammad Hossein Habibi*, Mosa Fakhrpor

Nanotechnology Laboratory, Department of Chemistry, University of Isfahan, Isfahan, 81746-73441 I.R. Iran, Tel. +98-313-7934914; Fax: +98-313-6689732; emails: habibi@chem.ui.ac.ir (M.H. Habibi), mousafakhrpoor1@gmail.com (M. Fakhrpor)

Received 25 March 2016; Accepted 22 July 2016

ABSTRACT

Cerium-zinc oxide nano-composite was synthesized by co-precipitation technique using zinc chloride ($ZnCl_2$), cerium (III) chloride hepta-hydrate ($CeCl_3.7H_2O$) and ammonium hydroxide as precipitation agent. The structural, morphological, thermal and spectroscopic properties of cerium-zinc oxide nano-composites were performed by Fourier transform infrared (FTIR), X-ray diffraction (XRD), field emission scanning electron microscopy (FESEM), transmission electron microscope (TEM), energy-dispersive analysis X-ray (EDAX) spectrometry, and UV–Vis diffuse reflectance spectroscopy (DRS) techniques. The FTIR spectra confirmed the presence of bands at 504 and 411 cm^{-1} are related to vibrations of Ce-O and Zn-O, respectively. The band at 886 cm^{-1} is due to the formation of Ce–O–Zn bond. The XRD result confirmed that the cerium-zinc oxide nano-composite obtained by co-precipitation technique possessed structure of cubic phase. The EDAX results confirmed the elemental distribution of cerium-zinc oxide nano-composite. The FESEM and TEM images showed sphere-like nano-particles that are agglomerated on the bulk-rods particles with an average size of about 31 nm. The DRS spectra of the cerium-zinc oxide nano-composite showed that absorption edge of ZnO was shifted to visible region. The optical band gap energy of the CeO_2-ZnO is measured to be 2.75 eV, which is relatively lower than that of bare ZnO (3.37 eV). The CeO_2-ZnO nano-composite showed higher degradation efficiency for photo-catalytic degradation of C.I. Acid Black 1 textile dye when compared with the bare ZnO and bare CeO_2. The reduced band gap energy lowered the rate of electron-hole pair recombination and increased the photo-catalytic degradation yield of dye pollutant.

Keywords: Cerium oxide; Zinc oxide; Nano-composite; Rare earths; Photo-catalytic mineralization

1. Introduction

CeO_2 is one of the main rare earths used in different industries for the catalytic degradation of environmental pollutants [1–3] and as a biomedical material with improved properties [4–6]. Nano-sized cerium dioxide plays an industrially significant role as exhaust catalysts, solid oxide fuel cells, gas sensors, ultraviolet absorbents and glass-polishing materials [7,8]. Zinc oxide as a semiconductor material has attracted wide research attention and applications because of its large direct band gap, non-toxicity, and abundance in nature [9,10]. Zinc oxide with a wide band gap (3.37 eV) absorbs photons in UV region of solar irradiation, while this UV irradiation make small portion of the solar light. The quantum yield of zinc oxide as photo-catalyst is low, which is related to its high electron-hole recombination rate. There are great needs to activate zinc oxide on the visible portion of solar irradiation and decrease its electron-hole recombination. The composite formation between zinc oxide and rare earth elements can activate zinc oxide on the visible portion of solar irradiation and decrease its electron-hole recombination [11,12]. Recently, the effects of CeO_2 coupling on the structural, optical and photo-catalytic properties of ZnO nano-particle have been reported [13]. There are some reports that photo-catalytic activity of cerium dioxide-titanium dioxide photo-catalyst decreased electron-hole recombination [3,14]. Among the

* Corresponding author.

different synthesis methods available, co-precipitation is a simple and inexpensive method for the industrial preparation of metal oxide catalysts [15]. Discharge of chemicals into the water systems can be harmful to aquatic life and need to be treated before their release into the environment. Among treatment methods, semiconductor photo-catalyst with band gap at visible solar irradiation has many advantages with a disadvantage of their application in the form of aqueous slurries, which encounter technological problems of recycling and separation from the slurry. This problem can be solved by coating of photo-catalyst on the support substrates [16]. The objectives of this research were to prepare and characterize the cerium-zinc oxide nano-composite and deposition on glass for photo-catalytic performance of aquatic pollutant degradation.

In continuation of our research in semiconductor metal oxide nano-structure materials [17–22], here we report for the first time the co-precipitation synthesis, structural, morphological, thermal and spectroscopic studies on cerium-zinc oxide nano-composite coated on glass surface for heterogeneous photo-catalytic mineralization of textile dye in aqueous environment. The structural, morphological, thermal and spectroscopic properties of cerium-zinc oxide nano-composites were investigated by FTIR, XRD, field emission scanning electron microscopy (FESEM), energy-dispersive analysis X-ray (EDAX), Thermogravimetric-derivative thermogravimetric (TG-DTG) analysis and diffuse reflectance spectroscopy (DRS) techniques. In order to overcome the problem of photo-catalyst separation from water system, cerium-zinc oxide nano-composites were coated on glass surface by doctor blade method. We have found that the cerium dioxide incorporation into zinc oxide lattice decreased the band gap energy of zinc oxide from 3.37 to 2.75 eV demonstrating its excitation energy at visible region of solar irradiation at 451 nm.

2. Experimental setup

2.1. Photo-catalyst synthesis

All reagents were of analytical grade and used as received without further purification. In a general co-precipitation preparation, 5 mmol of cerium (III) chloride heptahydrate ($CeCl_3.7H_2O$) (1.891 g) and 30 mmol zinc chloride ($ZnCl_2$) (4.238 g) were dissolved in 300 mL distilled water at room temperature and vigorously stirred for about 30 min for complete mixing. The pH was adjusted to 10 by dropwise addition of NH_4OH solution. The reaction mixture was then stirred at 80°C for 6 h. After the reactions, white solid precipitates were obtained, filtered and washed with water and ethanol several times and dried at room temperature. The resulting white powders were calcined at 400°C for 5 h (Fig. 1).

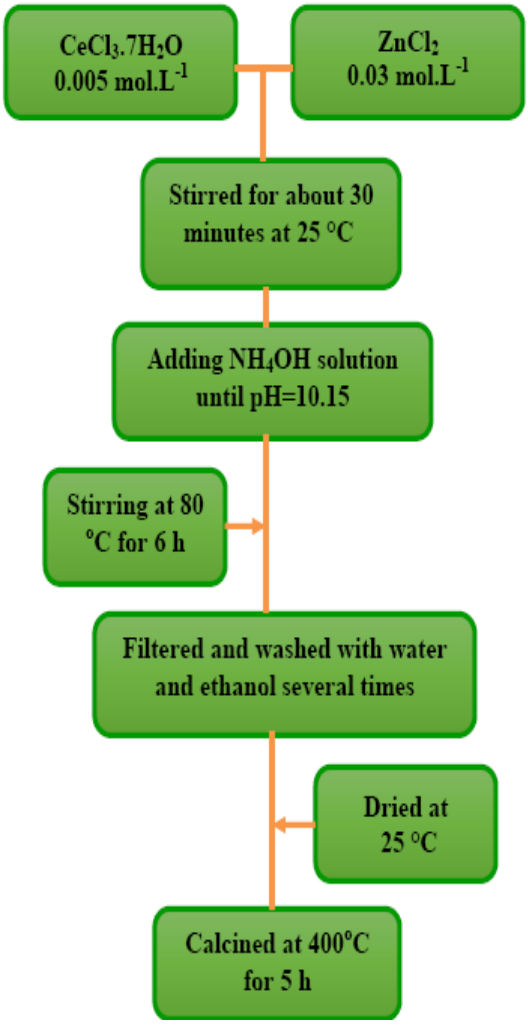

Fig. 1. Flow chart for preparation cerium-zinc oxide nano-composite particles by co-precipitation technique using zinc chloride ($ZnCl_2$), cerium (III) chloride hepta-hydrate ($CeCl_3.7H_2O$) and ammonium hydroxide as precipitation agent.

2.2. Coating thin film photo-catalyst on glass

Cerium-zinc oxide nano-composite was coated on borosilicate glass by doctor blade technique and spin coating method (Spin Coater, Modern Technology Development Institute, Iran) as follows: 130 μL of glacial acetic acid was added to 0.8 g of ZnO-CeO_2 powder and stirred for 5 min. Absolute ethanol (130 μL) was added and stirred for 1 min (15 times). Absolute ethanol (300 μL) was added for 1 min (6 times), sonicated for 2.5 min. Terpineol (0.8 mL) was added, and the paste solution were sonicated for 3 min (3 times). A solution of 0.4 g ethyl cellulose in 5 mL ethanol was sonicated for 3 min (3 times) and added to the previous paste solution, stirred for 5 min and sonicated for 3 min (3 times). The solvent was evaporated in a rotary evaporator at room temperature (r.t.). The paste of ZnO-CeO_2 nano-composite was coated on a glass slide (6 cm × 2 cm and 2 μm thickness) by doctor blade method, spin coating and annealed at 550°C for 2 h (Fig. 2).

2.3. Photo-catalyst characterization

The phase purity of the cerium-zinc oxide nano-composite thin films was characterized by X-ray diffraction (XRD) using X-ray diffractometer (D8 Advance, Bruker, Germany) with Cu Kα radiations (λ = 1.540562 Å) operated at voltage of 40 kV and current of 30 mA. The surface morphology of cerium-zinc oxide nano-composite thin films was analyzed by FESEM (Hitachi, S-4160, Japan). The chemical composition analysis of cerium-zinc oxide nano-composite was studied by energy-dispersive X-ray spectroscopy (EDXS) connected to the FESEM. Bang gap of cerium-zinc oxide nano-composite was

determined using diffuse reflectance spectroscopy (DRS) by a V-670 JASCO spectrophotometer and Munk relationship. A UV spectrophotometer (Varian Cary 500 Scan) was applied to analyze the pollutant dye concentrations. FTIR absorption spectra of cerium-zinc oxide nano-composites were obtained using KBr disks on a JASCO FT-IR 6300. The microstructure and morphologies were investigated by a Leo 912 AB transmission electron microscopy (TEM). Cerium-zinc oxide nano-composite thin films were coated on glass using doctor blade method and spin coating method (Spin Coater, Modern Technology Development Institute, Iran).

2.4. Photo-catalyst application

C.I. Acid Black 1 textile dye was chosen as a model pollutant of textile industry wastewater. The C.I. Acid Black 1 solution with a concentration of 20 ppm (calculated from the standard curve) was prepared as an initial dye solution.

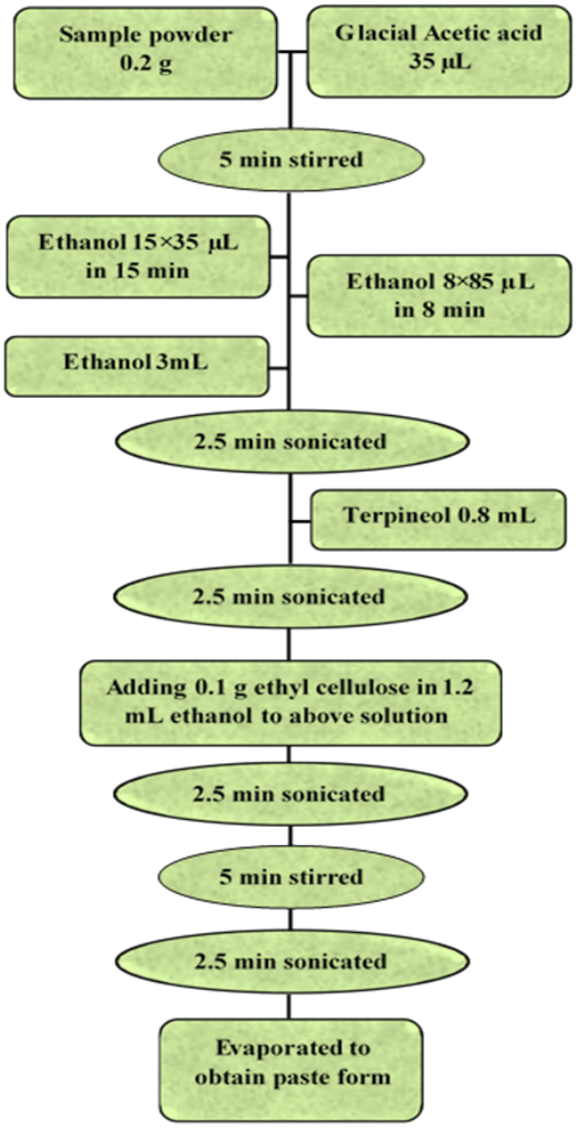

Fig. 2. Flow chart for coating of cerium-zinc oxide nano-composite on glass.

The dye solution exposed at O_2 gas for 20 min. Glass-coated cerium-zinc oxide nano-composite was immersed into a Petri dish with 20 mL of the dye solution and maintained at dark for 1 h. The reaction system illuminated by a 250-W Hg lamp at different times, and the concentration of the dye solution was determined by measuring the absorbance at 620 nm.

3. Results and discussion

3.1. Structural analysis

3.1.1. XRD study

Nano-particles were characterized by XRD analysis using X-ray diffractometer in the diffraction angle range 2θ = 10°–90° using Cu Kα radiation (λ = 1.540562 Å) operated at voltage of 40 kV and current of 30 mA. The crystallite size of the cerium-zinc oxide nano-composite was estimated by using the Scherer's equation, (0.9λ)/(βcosθ), by measuring the line broadening of main intensity peak, where λ is the wavelength of Cu Kα radiation, β is the full width at half-maximum (FWHM), and θ is the Bragg's angle. The crystalline structure and averaged crystal size is summarized in Table 1.

Table 1
XRD data of cerium-zinc oxide nano-composite particles by co-precipitation technique using zinc chloride ($ZnCl_2$), cerium (III) chloride hepta-hydrate ($CeCl_3.7H_2O$) and ammonium hydroxide as precipitation agent annealed at 400°C for 5 h

Phase	d-spacing (nm)	(hkl)	Phase	d-spacing (nm)	(hkl)
CeO_2	0.31100	(111)	ZnO	0.14769	(103)
ZnO	0.28159	(100)	ZnO	0.14071	(200)
ZnO	0.26019	(002)	ZnO	0.13790	(112)
ZnO	0.24760	(101)	ZnO	0.13590	(201)
CeO_2	0.19001	(220)	ZnO	0.19099	(102)
CeO_2	0.16200	(311)	ZnO	0.16099	(110)

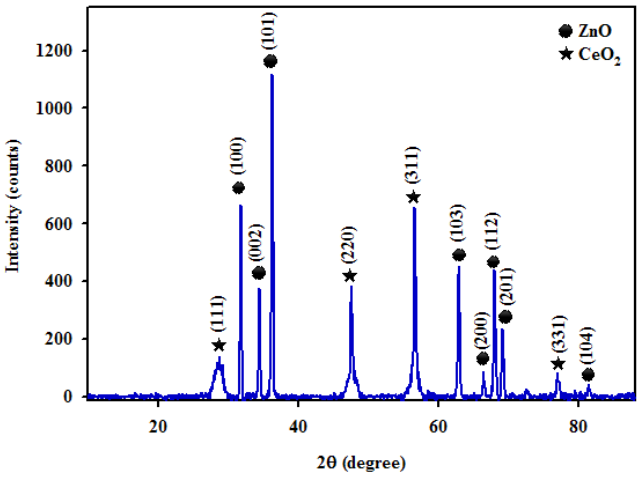

Fig. 3. XRD pattern of cerium-zinc oxide nano-composite particles by co-precipitation technique using $ZnCl_2$, $CeCl_3.7H_2O$ and ammonium hydroxide as precipitation agent annealed at 400°C for 5 h.

Fig. 3 shows the XRD patterns for the binary ZnO-CeO_2 nano-composite, which provide further insight into the crystallinity. The diffraction pattern matched the standard data for hexagonal zinc oxide and cubic cerium oxide phases. Lattice parameters for a hexagonal wurtzite zinc oxide (JCPDS 5-0664) were: a = b = 3.250 Å and c = 5.209 Å, $\alpha = \beta = 90°$ and $\gamma = 120°$. The result showed peaks attributed to the ZnO at d-spacing in nm = 0.28159 (100), 0.26019 (002), 0.24760 (101), 0.19099 (102), 0.16099 (110), 0.14769 (103), 0.14071 (200), 0.13790 (112) and 0.13590 (201). The XRD pattern consisted peaks for cubic cerium oxide (CeO_2) (JCPDS 1-0800) with lattice parameters at a = b = c = 5.41 and $\alpha = \beta = \gamma = 90°$. These results showed peaks attributed to the CeO_2 at 0.31100 (111), 0.19001 (220) and 0.16200 (311). The diffraction pattern matched the standard data for hexagonal wurtzite zinc oxide and cubic cerium oxide phases. The results showed a binary oxide nanostructure for the coupled ZnO-CeO_2 nano-composites, which consist of their characteristic peaks of both wurtzite ZnO and cubic phase CeO_2. The XRD results showed the characteristic peaks of both hexagonal wurtzite ZnO and cubic phase CeO_2, which is consistent with recent reports [23–25] (Fig. 3) (Table 1). The ionic radii of Ce^{3+} and Ce^{4+} are 0.103 and 0.092 nm, respectively, which are larger than that of Zn^{2+} ion of 0.074 nm reported by the others [23–28]. Hence, it is difficult for Ce^{3+} and Ce^{4+} to enter the crystalline lattice of ZnO to substitute Zn^{2+}. The Ce^{3+} and Ce^{4+} ions seem more likely to form complex with the surface oxygen of ZnO. The presence of redox couple Ce^{3+}/Ce^{4+} could enhance the photo-catalytic of the ZnO-CeO_2 nano-composite, which acts as an electron scavenger, and photogenerated electrons in conduction band (CB) of ZnO are transferred to CB of CeO_2 and reduce the rate of electron/hole recombination [23,29].

3.1.2. Fourier transform infrared (FTIR) study

The chemical structure of the cerium-zinc oxide nano-composite prepared by co-precipitation method from chloride precursor and calcined at 400°C was ascertained by the FTIR spectroscopy. The FTIR spectroscopy of cerium-zinc oxide nano-composite was recorded on JASCO FT-IR 6300 spectrometer using KBr pellet. The FTIR spectra were recorded at room temperature in the wave number range of 500–4,000 cm^{-1}. The FTIR spectra of the above sample are shown in Fig. 4. The band positions at 3,435 cm^{-1} were attributed to the characteristic O-H stretching vibrations. The peak is observed at 3,435 cm^{-1} due to O-H stretching vibrations interacting through H bonds. The absorption bands observed at 504 and 411 cm^{-1} are related to stretching vibrations of Ce-O and Zn-O, respectively. The band at 886 cm^{-1} is due to the formation of Ce–O–Zn bond. All characteristic peaks in FTIR spectrum were analyzed and confirmed the formation of cerium-zinc oxide composite phase (Fig. 4).

3.2. Microstructural analysis

3.2.1. FESEM study

The surface morphology of the cerium-zinc oxide nano-composite was performed with the aid of FESEM. Fig. 5 shows the FESEM image of the glass deposited cerium-zinc

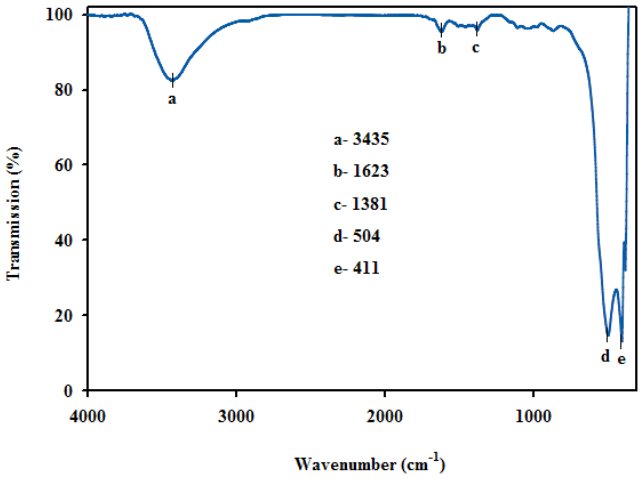

Fig. 4. FTIR spectra of cerium-zinc oxide nano-composite particles by co-precipitation technique using $ZnCl_2$, $CeCl_3.7H_2O$ and ammonium hydroxide as precipitation agent annealed at 400°C for 5 h.

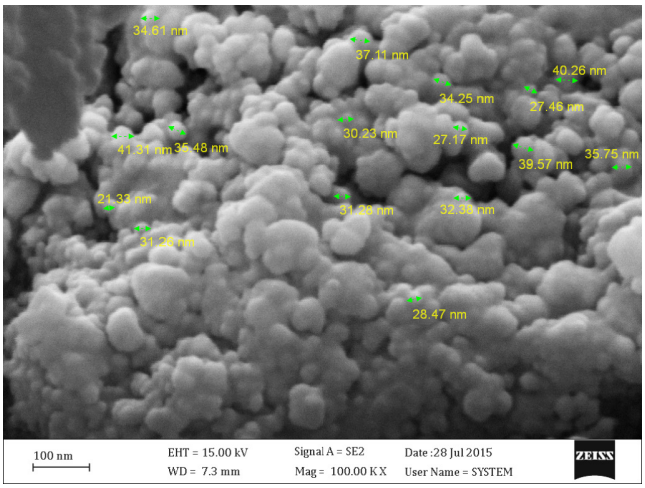

Fig. 5. FESEM image of cerium-zinc oxide nano-composite particles by co-precipitation technique using $ZnCl_2$, $CeCl_3.7H_2O$ and ammonium hydroxide as precipitation agent annealed at 400°C for 5 h.

oxide nano-composite calcined at 400°C for 5 h. It is observed that the surfaces consist of sphere-like nano-particles that are agglomerated on the bulk-rods particles. The average size of nano-particles is about 40 nm (Fig. 5).

3.3. Compositional analysis

Fig. 6 shows the elemental analysis of cerium-zinc oxidenano-composite confirmed by EDAX. In the EDAX pattern, presence of Ce, Zn and O showed that expected elemental analysis was observed (Fig. 6). The EDAX results also proved that the precursors used for the preparation have fully undergone the chemical reaction to form the cerium-zinc oxide nano-composite. Particle size distribution showed the average particle size of 31 nm (Fig. 7).

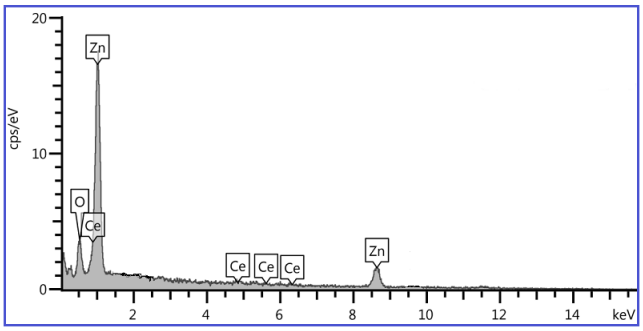

Fig. 6. EDAX pattern of cerium-zinc oxide nano-composite particles by co-precipitation technique using $ZnCl_2$, $CeCl_3.7H_2O$ and ammonium hydroxide as precipitation agent annealed at 400°C for 5 h.

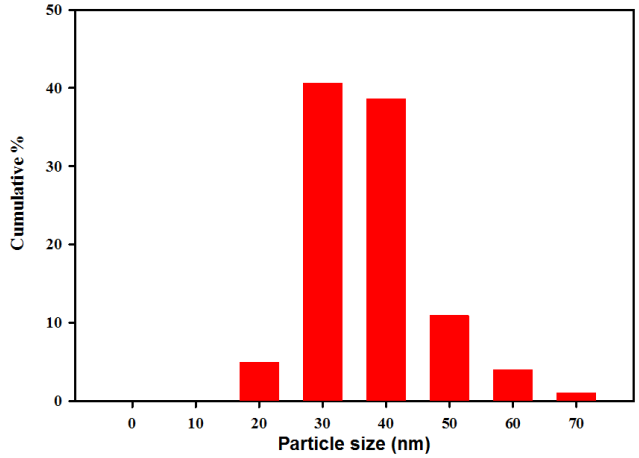

Fig. 7. Particles distribution of cerium-zinc oxide nano-composite particles by co-precipitation technique using $ZnCl_2$, $CeCl_3.7H_2O$ and ammonium hydroxide as precipitation agent annealed at 400°C for 5 h.

3.4. TEM study

Fig. 8 shows a typical TEM micrograph of the synthesized cerium-zinc oxide nano-composite coated on glass. We have found that cerium-zinc oxide nano-composites were affiliated well on the surface of glass with an average size of 33 nm.

3.5. Optical study by ultraviolet–visible DRS (UV–Vis DRS) analysis

UV–Vis DRS is a powerful characterization method to study the band gap energy of semiconductors. The absorption spectrum of solid cerium-zinc oxide nano-composite was shown in Fig. 9. The band gap of the cerium-zinc oxide nano-composite was estimated using Kubelka–Munk plot (Fig. 10). The band gap was calculated by extrapolating the linear region of the plot [30]. The band gap was determined to be 2.75 eV. The optical band gap energy of the CeO_2-ZnO is relatively lower than that of bare ZnO (3.37 eV).

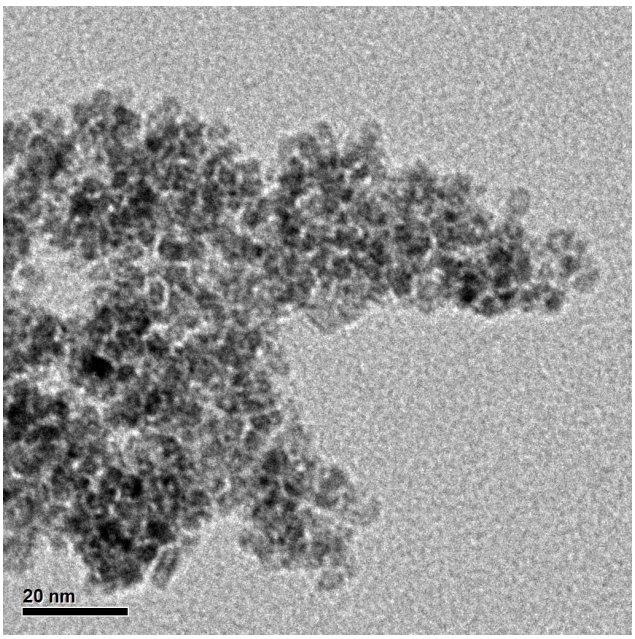

Fig. 8. Transmission electron microscopy (TEM) of cerium-zinc oxide nano-composite particles by co-precipitation technique using $ZnCl_2$, $CeCl_3.7H_2O$ and ammonium hydroxide as precipitation agent annealed at 400°C for 5 h.

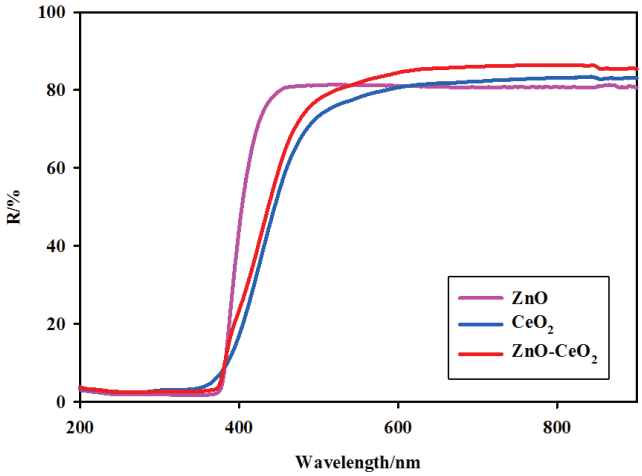

Fig. 9. UV–Vis diffuse reflectance spectroscopy (DRS) absorption spectra of cerium-zinc oxide nano-composite particles by co-precipitation technique using $ZnCl_2$, $CeCl_3.7H_2O$ and ammonium hydroxide as precipitation agent annealed at 400°C for 5 h.

3.6. Photo-catalytic degradation and mechanism

Photo-catalytic degradation of C.I. Acid Black 1 for different irradiation times and the change in optical absorption spectra of C.I. Acid Black 1 by cerium-zinc oxide nano-composite coated on glass is shown in Fig. 11. The disappearance of the band at 610 nm indicates that C.I. Acid Black 1 (Fig. 11) has been photo-degraded. CeO_2-ZnO nano-composite coated on glass surface by doctor blade method provided an effective way for cost-effective, simple and fast process. Fig. 12 shows

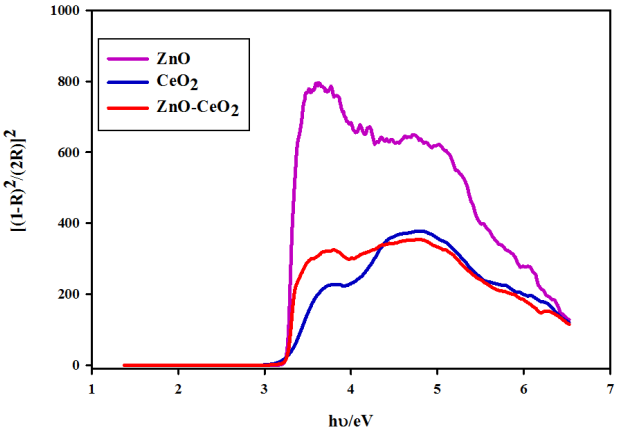

Fig. 10. Munk plot derived from UV–Vis DRS spectra of cerium-zinc oxide nano-composite particles by co-precipitation technique using $ZnCl_2$, $CeCl_3.7H_2O$ and ammonium hydroxide as precipitation agent annealed at 400°C for 5 h.

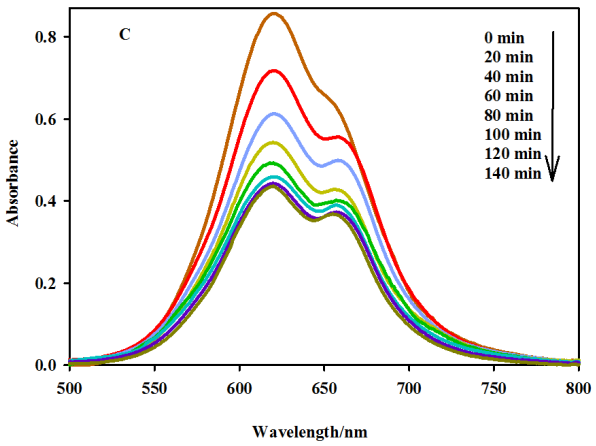

Fig. 11. Time-dependent absorption spectra of C.I. Acid Black 1 for different irradiation times using cerium-zinc oxide nano-composite particles coated on glass as photo-catalyst.

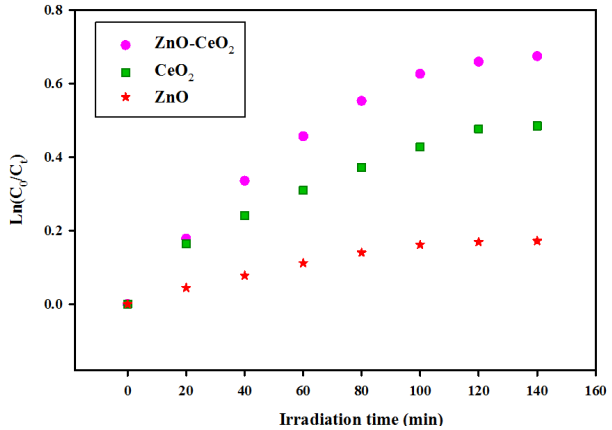

Fig. 12. Ln (C_0/C_t) vs. time (min) for the photo-catalytic degradation kinetics of the C.I. Acid Black 1 for different irradiation times using cerium-zinc oxide nano-composite particles coated on glass as photo-catalyst.

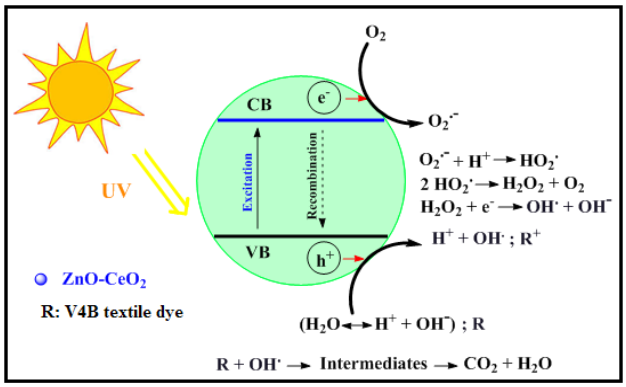

Fig. 13. Schemes for the photo-catalytic degradation mechanisms of C.I. Acid Black 1 using cerium-zinc oxide nano-composite particles coated on glass as photo-catalyst.

the photo-catalytic degradation kinetics of the C.I. Acid Black 1 under irradiation in the presence of pure CeO_2, pure ZnO and ZnO-CeO_2 nano-composite prepared by co-precipitation method from chloride precursor as thin films photo-catalyst. The CeO_2-ZnO nano-composite shows higher degradation efficiency when compared with the bare ZnO and bare CeO_2. Zinc oxide is a p-type semiconductor, and cerium dioxide is an n-type material. Fig. 13 shows photo-catalytic reaction schemes for degradation of dye molecule. Upon irradiation of cerium-zinc oxide nano-composite under UV light, both cerium oxide and zinc oxide can be activated with the band gap energies of zinc oxide and cerium oxide, which are 3.37 and 1.38 eV, respectively. Photo-catalytic degradation of C.I. Acid Black 1 in the presence of pure ZnO nano-particles are lower than the CeO_2-ZnO nano-composite due to the value of 3.37 eV band gap of ZnO. In the photo-catalytic mechanism, oxygen adsorbed on the surface of photo-catalyst can trap the photo-generated electron [31] and the electron transfer to oxygen may be the rate-determining step in semiconductor photo-catalysis [32]. Cerium (IV) ion as a Lewis acid traps the photo-excited electron in the system of CeO_2-ZnO, since it is superior to the oxygen molecule in the ability of trapping electrons [33]. The electrons trapped in cerium (IV) ion are then transferred to the adsorbed oxygen molecule by oxidation process, which reduced electrons-holes recombination [34].

4. Conclusions

Cerium-zinc oxide nano-composite coated on glass was prepared by co-precipitation technique using $ZnCl_2$, cerium (III) chloride hepta-hydrate and ammonium hydroxide as precipitation agent. The structural, morphological, thermal and spectroscopic properties of cerium-zinc oxide nano-composites were performed by FTIR, XRD, FESEM, EDAX, TG-DTG and DRS techniques. The FTIR spectra confirmed the presence of bands related to vibrations of Ce-O, Zn-O and Ce–O–Zn bonds. The XRD results confirmed that the cerium-zinc oxide nano-composite possessed structure of cubic phase. The EDAX results confirmed the elemental distribution of cerium-zinc oxide nano-composite. The FESEM images showed sphere-like nano-particles that are agglomerated on the bulk-rods particles with an average size of

about 31 nm. The DRS spectra of the cerium-zinc oxide nanocomposite showed that absorption edge of ZnO was shifted to visible region. The optical band gap energy of the CeO_2-ZnO is measured to be 2.75 eV, which is relatively lower than that of bare ZnO (3.37 eV). The reduced band gap energy lowered the rate of electron-hole pair recombination and increased the photo-catalytic degradation yield of dye pollutant.

Acknowledgment

The authors wish to thank the University of Isfahan for financially supporting this work.

References

[1] P. Phatai, C.M. Futalan, Removal of methyl violet dye by adsorption onto mesoporous mixed oxides of cerium and aluminum, Desal. Wat. Treat., 57 (2016) 8884–8893.
[2] H. Eskandarloo, A. Badiei, M.A. Behnajady, Application of response surface methodology for optimization of operational variables in photodegradation of phenazopyridine drug using TiO_2/CeO_2 hybrid nanoparticles, Desal. Wat. Treat., 54 (2015) 3300–3310.
[3] T. Zhang, Q. Li, Z. Mei, H. Xiao, H. Lu, Y. Zhou, Adsorption of fluoride ions onto non-thermal plasma-modified CeO_2/Al_2O_3 composites, Desal. Wat. Treat., 52 (2014) 3367–3376.
[4] X. Song, L. Wang, M. Niinomi, M. Nakai, Y. Liu, M. Zhu, Microstructure and fatigue behaviors of a biomedical Ti–Nb–Ta–Zr alloy with trace CeO_2 addition, Mater. Sci. Eng., A, 619 (2014) 112–118.
[5] W.J. Shan, H.J. Guo, C. Liu, X.N. Wang, Controllable preparation of CeO_2 nanostructure materials and their catalytic activity, J. Rare Earths, 30 (2012) 665–669.
[6] M.J. Akhtar, M. Ahamed, H.A. Alhadlaq, M.A.M. Khan, S.A. Alrokayan, Glutathione replenishing potential of CeO_2 nanoparticles in human breast and fibrosarcoma cells, J. Colloid Interface Sci., 453 (2015) 221–227.
[7] L. He, Y. Su, J. Lanhong, S. Shi, Recent advances of cerium oxide nanoparticles in synthesis, luminescence and biomedical studies: a review, J. Rare Earths, 33 (2015) 791–799.
[8] Q. Xie, Y. Zhao, H. Guo, A. Lu, X. Zhang, L. Wang, M.-S. Chen, D.-L. Peng, Facile preparation of well-dispersed CeO_2–ZnO composite hollow microspheres with enhanced catalytic activity for CO oxidation, ACS Appl. Mater. Interfaces, 6 (2014) 421–428.
[9] E. Castillejos, R. Bacsa, A.G. Ruiz, L. Datas, P. Serp, Catalytic activity of gold supported on ZnO tetrapods for the preferential oxidation of carbon monoxide under hydrogen rich conditions, Nanoscale, 3 (2011) 929–932.
[10] F. Du, N. Wang, D. Zhang, Y. Shen, Preparation, characterization and infrared emissivity study of Ce-doped ZnO films, J. Rare Earths, 28 (2010) 391–395.
[11] J.-C. Sin, S.-M. Lam, K.-T. Lee, A.R. Mohamed, Preparation of rare earth-doped ZnO hierarchical micro/nanospheres and their enhanced photocatalytic activity under visible light irradiation, Ceram. Int., 40 (2014) 5431–5440.
[12] X.J. Zhang, W.B. Mi, X.C. Wang, H.L. Bai, First-principles prediction of electronic structure and magnetic ordering of rare-earth metals doped ZnO, J. Alloys Compd., 617 (2014) 828–833.
[13] E.D. Sherly, J.J. Vijaya, L.J. Kennedy, Effect of CeO_2 coupling on the structural, optical and photocatalytic properties of ZnO nanoparticle, J. Mol. Struct., 1099 (2015) 114–125.
[14] X. Zhuo, Y.C. Zhao, J.Y. Zhang, C.G. Zheng, Efficient photocatalytic reduction of CO_2 into liquid products over cerium doped titania nanoparticles synthesized by a sol-gel auto-ignited method, Fuel Process. Technol., 135 (2014) 6–13.
[15] P. Sathishkumar, R.V. Mangalaraja, T. Pandiyarajan, R. Garcia, Low frequency ultrasound assisted sequential and co-precipitation syntheses of nanoporous RE (Gd and Sm) doped cerium oxide, RSC Adv., 5 (2015) 22578–22586.
[16] M.H. Habibi, J. Parhizkar, Cobalt ferrite nano-composite coated on glass by doctor blade method for photo-catalytic degradation of an azo textile dye Reactive Red 4: XRD, FESEM and DRS investigations, Spectrochim. Acta, Part A, 150 (2015) 879–885.
[17] M.H. Habibi, M. Mardani, Effect of annealing temperature on optical properties of binary zinc tin oxide nano-composite prepared by sol–gel route using simple precursors: structural and optical studies by DRS, FT-IR, XRD, FESEM investigations, Spectrochim. Acta, Part A, 137 (2015) 267–270.
[18] M.H. Habibi, M. Mardani, Co-precipitation synthesis of nano-composites consists of zinc and tin oxides coatings on glass with enhanced photocatalytic activity on degradation of Reactive Blue 160 KE2B, Spectrochim. Acta, Part A, 137 (2015) 785–789.
[19] M.H. Habibi, E. Askari, Fabrication and spectral properties of zinc zirconate nanorod composites by sol-gel method for optical applications: effect of chloride and oxychloride precursors and sintering temperature on band gap, Synth. React. Inorg. Met.-Org. Chem., 45 (2015) 281–285.
[20] M.H. Habibi, Z. Rezvani, Photocatalytic degradation of an azo textile dye (C.I. Reactive Red 195 (3BF)) in aqueous solution over copper cobaltite nanocomposite coated on glass by doctor blade method, Spectrochim. Acta, Part A, 147 (2015) 173–177.
[21] M.H. Habibi, M.H. Rahmati, The effect of operational parameters on the photocatalytic degradation of Congo red organic dye using ZnO–CdS core–shell nano-structure coated on glass by doctor blade method, Spectrochim. Acta, Part A, 137 (2015) 160–164.
[22] M.H. Habibi, E. Askari, Preparation of a novel zinc zirconate nanocomposite coated on glass for removal of a textile dye (Reactive Brilliant Red X8B) from water, Synth. React. Inorg. Met.-Org. Chem., 45 (2015) 1457–1462.
[23] M. Yousef, M. Amiri, R. Azimirad, A.Z. Moshfegh, Enhanced photoelectrochemical activity of Ce doped ZnO nanocomposite thin films under visible light, J. Electroanal. Chem., 661 (2011) 106–112.
[26] J. Yang, M. Gao, L. Yang, Y. Zhang, J. Lang, D. Wang, Y.W.H. Liu, H. Fan, Low-temperature growth and optical properties of Ce-doped ZnO nanorods, Appl. Surf. Sci., 255 (2008) 2646–2650.
[27] G.-R. Li, X.-H. Lu, W.-X. Zhao, C.-Y. Su, Y.-X. Tong, Controllable electrochemical synthesis of Ce^{4+}-doped ZnO nanostructures from nanotubes to nanorods and nanocages, Cryst. Growth Des., 8 (2008) 1276–1281.
[28] J.-H. Yang, M. Gao Y.-J. Zhang, L.-L. Yang, Synthesis and optical properties of Ce-doped ZnO, Chem. Res. Chin. Univ., 24 (2008) 266–269.
[29] R.E. Marotti, D.N. Guerra, C. Bello, G. Machado, E.A. Dalchiele, Bandgap energy tuning of electrochemically grown ZnO thin films by thickness and electrodeposition potential, Sol. Energy Mater. Sol. Cells, 82 (2004) 85–103.
[30] D. Das, R.K. Dutta, A novel method of synthesis of small band gap SnS nanorods and its efficient photocatalytic dye degradation, J. Colloid Interface Sci., 457 (2015) 339–344.
[31] Z. Li, Y. Luan, Y. Qu, L. Jing, Modification strategies with inorganic acids for efficient photocatalysts by promoting the adsorption of O_2, ACS Appl. Mater. Interfaces, 7 (2015) 22727–22740.
[32] B. Ohtani, Titania photocatalysis beyond recombination: a critical review, Catalysts, 3 (2013) 942–953.
[33] B. Subash, B. Krishnakumar, R. Velmurugan, M. Swaminathan, M. Shanthi, Synthesis of Ce co-doped Ag–ZnO photocatalyst with excellent performance for NBB dye degradation under natural sunlight illumination, Catal. Sci. Technol., 2 (2012) 2319–2326.
[34] C. Sun, H. Li, L. Chen, Nanostructured ceria-based materials: synthesis, properties, and applications, Energy Environ. Sci., 5 (2012) 8475–8505.